Optics & Laser Technology 67 (2015) 137–142

Contents lists available at ScienceDirect

Optics & Laser Technology

journal homepage: www.elsevier.com/locate/optlastec

Corrosion monitoring of rock bolt by using a low coherent fiber-optic interferometry

Heming Wei [a], Xuefeng Zhao [b,*], Dongsheng Li [b], Pinglei Zhang [a], Changsen Sun [a,**]

[a] College of Physics and Optoelectronic Engineering, Dalian University of Technology, Dalian 116024, China
[b] State Key Laboratory of Coastal and Offshore Engineering, Dalian University of Technology, Dalian 116024, China

ARTICLE INFO

Article history:
Received 13 May 2014
Received in revised form
29 September 2014
Accepted 4 October 2014
Available online 6 November 2014

Keywords:
Corrosion monitoring
Rock bolt
Low-coherent fiber-optic sensor

ABSTRACT

Corrosion of rock bolts is a major cause for deterioration of the anchor-reinforced concrete slopes structures. In order to evaluate this corrosion-based deterioration in an early stage, a nondestructive technique was required. However, until now, there are no commercialized solutions that are straightforwardly available. Here, a low-coherent fiber-optic sensing technique was developed. This method can carry out the monitoring of the corrosion-caused expansion at the accuracy of sub-microstrains by circled the sensing optical fiber in two ways. One was wound the fiber on the surface of steel rock bolt directly, and thereby generated a nonuniformity in the interface of cement with rock bolt. The other was circled the fiber on a cement mortar cushion without destroying the interface any way. The sensing fiber was configured as one arm of the fiber-optic Michelson interferometer. The acceleration corrosion experiments demonstrated that a uniform interface between cement and rock bolt determined the progress of corrosion development. An early stage evaluation of the corrosion development in rock bolts was monitored.

1. Introduction

Rock bolt was popular, economical and successful choice for slope stability. It anchored to prevent the slopes from the destruction of landslide, earthquake, and other natural disasters. The corrosion in rock bolt was a major cause to deteriorate the structures. Some methods were proposed to evaluate this progress by monitoring the displacement [1–4], tension levels [5,6], settlement [7], etc. However, these macro scale method could not meet the requirement of evaluating the structure deterioration in their early stage. And, this was a kernel problem in many cases, such as in the high speed rail ways related structures [8].

The common understanding about the corrosion development was that the anchor-reinforced concrete structures were suffering an alkaline condition, which would lead to form a passive layer on the anchor surface, and thereby prevented the rock bolt from a further corrosion [9]. The further corrosion was happened accompanying several chemical reactions on the anchor surface [10]. The chemical resultants, especially the ferrous ion Fe^{2+} and chloride ions can break down the passive layer and cause a further deterioration in the structures [11]. Thus an inner corrosion of a structure monitoring method was necessary to carry out an early prediction on its corrosion progress. And it was not likely to be simply related the corrosion of rock bolts to a crack [9,12], because there was a large gap between an inner corrosion happening and an observed macro-scale crack.

Many efforts had been made to achieve this goal. Electrochemical techniques [13] measured the corrosion development based the ionic concentration accumulated on the surface of the concrete structure. It will not be a very early method, because that the ions diffusing to the concrete surface was a time consuming process. Surely, it was preceded to the crack method. Acoustic emission technique [14,15] was aiming to explore the interface directly, but its resolution was limited in one of the wavelength of the employed acoustic waves, which was typically in the range of 0.2–200 mm correspond to the frequencies from 20 kHz to 20 MHz [16] and the velocity in concrete was about 4 km/s. Optical sensing technique was relatively practical for long-term monitoring. Habib et al. [17] developed an optical corrosion meter based on the holographic interferometry to measure the corrosion happening in different metallic samples emerged in the corrosive solutions. Mayorga-Cruz et al. [18] reported a method in Michelson interferometric configuration to realize the monitoring and evaluation of the corrosion processes in the distilled water. These methods were limited in monitoring corrosion outside of the structure, and therefore they cannot implement an early monitoring mentioned above.

* Corresponding author. Tel.: +86 411 8470 6443; fax: +86 411 84706414.
** Corresponding author. Tel.: +86 411 8470 7082; fax: +86 411 84709304.
E-mail addresses: hmwei@mail.dlut.edu.cn (H. Wei), zhaoxuefeng1977@gmail.com (X. Zhao), lidongsheng@dlut.edu.cn (D. Li), zpl200421013@gmail.com (P. Zhang), suncs@dlut.edu.cn (C. Sun).

http://dx.doi.org/10.1016/j.optlastec.2014.10.004
0030-3992/

Here, we proposed a method to monitor the corrosion-caused strain in the rock bolt based on the fact that the early-stage corrosion must generate a volume expansion and this strain was too weak to produce a crack, but it could be detected by using a fiber-optic interferometric method.

2. Theory background

Fig. 1 showed the schematic diagram of an array low-coherent fiber-optic sensor (A-LCFS) system for corrosion monitoring of rock bolts. The principle was based on a fiber-optic Michelson interferometer and multiplexed by a $1 \times N$ optical switch.

The light from a super-luminescent emitting diode (SLED) source, with a center wavelength of 1310 nm and a bandwidth of 45 nm, was coupled to a $1 \times N$ optical switch through a circulator C. The light of the first switched arm is transmitted through a half-reflection mirror (HM) to the sensing fiber 1 and reflected by a total-reflection mirror (TM) after suffering from a time delay τ_1. Both the half- and total-reflection lights were combined and coupled back into the optical switch as shown in the sensing part of Fig. 1 and incident to a 3 dB 2×2 coupler in the demodulation part through the receiver port of the circulator C, which can be described by: $E_0(\tau)+E_0(\tau+\tau_1)$. Where $E_0(\tau)$ represented as the light from HM and $E_0(\tau+\tau_1)$ stood for that from TM. $\tau_1=2nl_i/c$ described the time delay by the length of the sensing fiber l_i, which were indicated as 1, 2, …, N in Fig.1. c was the velocity of light in vacuum. A linear stepping stage was utilized as the scanning arm, by which the variable path length of the Michelson interferometer was carried out. The light was collimated into a parallel light a shelf focus lens, projected to the scanning mirror and then reflected back to the self-focus lens. The other arm of the 3 dB coupler was connected with a mirror and formed a fixed arm. The scanning mirror created a variable path length and formed a corresponding path difference with the fixed arm, in order to make these path differences being equivalent to the path lengths of the sensing fibers, respectively.

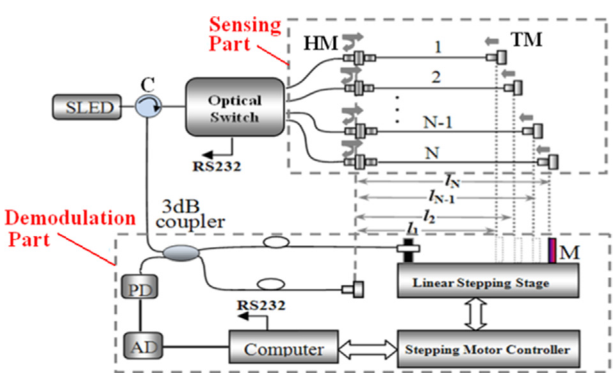

Fig. 1. Configuration of the A-LCFS system. SLED—super-luminescent emitting diode, C—circulator, RS232—the series port for computer communication. PD—photodetector, AD—Analog digital convertor, M—total-reflection moving mirror, HM—half-reflection mirror, TM—total-reflection mirror.

The signal from the circulator C was incident into the 3 dB coupler and was equally separated into two paths. The lights propagated in the two arms were reflected by the fixed mirror and the scanning mirror, respectively, and approached the photo-detector (PD). Finally, the output signal on PD can be described as:

$$E(\tau)=1/2 \times [E_0(\tau)+E_0(\tau+\tau_1)+E_0(\tau+\tau_2)+E_0(\tau+\tau_1+\tau_2)] \quad (1)$$

where $\tau_2=2l_x/c$, l_x is corresponding to the optical path determined by the position of the scanning motor. Then, the optical intensity detected by the PD could be represented as:

$$I=|E(\tau)|^2=E(\tau)E^*(\tau)=I_0+I(\tau_1)+I(\tau_2)+I(\tau_1+\tau_2)+I(\tau_1-\tau_2) \quad (2)$$

The first term I_0 was direct current (DC) and $I(\tau_1)$, $I(\tau_2)$, $I(\tau_1+\tau_2)$ and $I(\tau_1-\tau_2)$ were indicated the interference terms. $I(\tau_1-\tau_2)$ was the only interference term detected by the PD as an alternating current (AC) among all the phase differences formed by the time delays τ_1, τ_2, $\tau_1+\tau_2$ and $\tau_1-\tau_2$, respectively, and could be expressed as:

$$I_D=I(\tau_1-\tau_2)=1/4 \times [E_0(\tau+\tau_2)E_0^*(\tau+\tau_1)+E_0(\tau+\tau_1)E_0^*(\tau+\tau_2)] \quad (3)$$

when τ_2 was equivalent to τ_1 as the same principle given in Ref. [11], the position of the movement of scanning mirror could find an equivalent path length corresponding to the selected sensing fiber. The interference fringes were obtained as shown in Fig. 2(a).

In order to analyze this detected signal, we read the positions of the scanning motor, zoomed in the central peak of the interference fringe and showed in Fig. 2(b). Based on a data fitting processing [19,20], the precise central interference position was obtained with a resolution of the motor position readout within 5 μm, which was determined by the accuracy of stepping motor 1.25 μm/step underlying the interference condition of $\tau_2=\tau_1$.

When the length of the sensing fiber was somehow deformed, the corresponding interference position x_i would be thereby changed to a new position x'_i. Hence, the deformation in the sensing fiber l_i could be given by:

$$\Delta l_i=|x_i-x'_i|L_{step}/n \quad (4)$$

where n was the effective refractive index of the sensing fiber, l_i was the length of the corresponding sensing fiber, and $L_{step}=1.25$ μm presented the accuracy of the stepping motor. And then, the

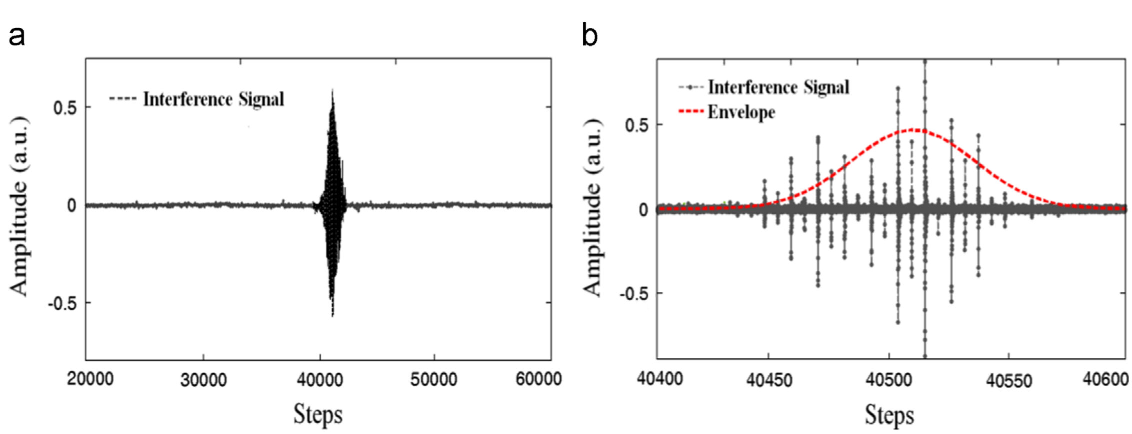

Fig. 2. A practical measured interference fringe and signal processing. (a) A practical measured interference fringe, (b) Zoom in the fringe showed in (a) and make a fitting processing.